

Analysis of specimen composition with the complex method using the backscattered electrons

DANUTA KACZMAREK, ANDRZEJ DETKA

Faculty of Microsystem Electronics and Photonics, Wrocław University of Technology, Wybrzeże Wyspiańskiego 27, 50-370 Wrocław, Poland.

For the investigation of different types of welds joined with electron beam the methods like the X-ray microanalysis or microscopic examination of cross-sections are usually employed. The work presents the improved method of specimen composition analysis with backscattered electron signal (BSE) in the scanning electron microscope (SEM). The method consists in: the application of the separation of information about composition and topography of examined specimens by introducing a correction term into the algorithm of COMPO mode creation, the linearization of backscattering coefficient characteristics *versus* an atomic number and application of colour simulation. The verification of obtained results has been done on the example of W-Mo weld by typical methods employed in metallography.

1. Introduction

The method employing backscattered electron signal (BSE) in a scanning electron microscope (SEM), used for the examination of material composition of a specimen, can be competitive in comparison with other methods for material composition evaluation, basing on the X-ray [1], [2] or Auger electrons analysis [3]. The successful application of the BSE signal in medical or biological diagnostics justifies such a statement [4]–[6]. The main advantages of employing the BSE signal to material analysis consist mainly in the accuracy, fast response and the possibility of analysing elements with low atomic numbers [7], [8].

The application of the BSE signal for the creation of the map of surface material composition is possible due to almost linear dependence of η coefficient of backscattered electrons (where η is defined as intensity of the backscattered electrons to intensity of the primary electrons ratio) on the atomic number Z of the examined element. But the material resolution ΔZ (where ΔZ is the smallest difference in atomic numbers between adjacent elements possible to be distinguished in the SEM image) decreases for $Z > 40$, because the coefficient η reaches its almost saturation value [9]. In our previous paper the method of enhancement of SEM resolution in the case of material contrast by linearization of backscattering characteristics $\eta = f(Z)$ was proposed [10].

The accuracy of material analysis in the BSE method is determined by the quality of black and white digital image [11]–[14]. As it is commonly known, the

BSE signal contains the information both on the specimen topography and composition [15], [16]. The simplest way of separating both pieces of information is an appropriate arrangement of a multi-detector system in relation to the specimen surface [17]–[20] and application of an appropriate algorithm for signal processing [21], [22]. The composition image is usually created as a sum of BSE signals from the detectors located at a certain height over the specimen surface. The digital image prepared in such a way is called the COMPO mode. On the other hand, the topography image is typically created as the difference of signals from two detectors located symmetrically along the primary beam (TOPO mode).

In order to expand the diagnostic possibilities of a typical SEM, the complex method for the COMPO mode has been proposed. The method consists of the following stages:

- recording of microscopic images in the form of digital bitmap,
- separation of the TOPO and COMPO modes according to the original theory [23],
- correction of the COMPO mode based on a theoretical analysis,
- linearization of BSE detector characteristics [23],
- simulation of colours for specimen composition analysis.

2. Separation of the TOPO and COMPO modes in SEM

As it has been already mentioned, one of the basic problems connected with the creation of the SEM image with BSE signal is the fact that the signal contains the information about both material composition and topography of the specimen. The improvement of various methods of surface image reconstruction is related closely to two theoretical ways of solving the problem. The first one consists in the development of a theory concerning the description of backscattered electrons phenomenon itself [24], whereas the second one tends to the elaboration of appropriate algorithms for mixing the signals from four detectors [21].

The improved COMPO mode due to a better separation of both the topographic and material contrasts in SEM has been obtained with the use of a simplified model. According to MURATA [25], who combined Rutherford's law of scattering with Everhart's model of single-scattering and Thomson–Whiddington's law of energetic losses, the BSE current density after some transformations [23] takes the form

$$j(A, \alpha) = j_A dA + j_\alpha d\alpha + \frac{1}{2!} [j_{AA} (dA)^2 + 2j_{A\alpha} dA d\alpha + j_{\alpha\alpha} (d\alpha)^2] \quad (1)$$

where: A – information carrier about the kind of material, α – information carrier about surface topography, $j_A, j_\alpha, j_{AA}, j_{\alpha\alpha}, j_{A\alpha}$ – partial derivatives expanded into Taylor's series for the function of two variables A and α . In Equation (1) the component $j_A dA$ contains the information about material in the dA factor, the component $j_\alpha d\alpha$ – the information about topography in the $d\alpha$ factor.

For the TOPO mode, when the signals from single detectors are subtracted, the terms with the even power α disappear, whereas the terms containing the factor

$dA d\alpha$ remain as a disturbance signal which can be called the COMPO·TOPO. This disturbance term of the opposite sign has been used to obtain the corrected TOPO mode.

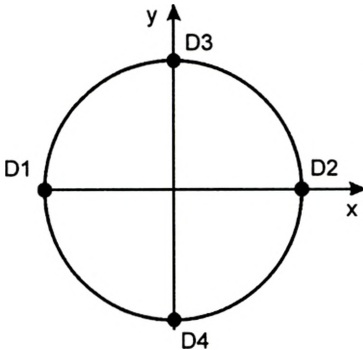


Fig. 1. Arrangement of four semiconductor detectors in the xy co-ordinate system. These detectors were located under the objective lens of the microscope.

For the COMPO mode, when the signals from single detectors should be added, the terms with the odd power α disappear. However, the term containing the factor $d\alpha^2$ remains as a disturbance signal and it can be called the TOPO². This disturbance term of the opposite sign has been used to obtain the corrected COMPO mode.

Basing on theoretical considerations [23], the method of separating the COMPO mode in SEM by compensation of disturbance signals has been proposed. From the developed theory of separation it follows that the COMPO mode, generated as the sum of signals from $D1$ and $D2$ detectors (Fig. 1), is disturbed by the signal which can be defined with the expression in the form of $\alpha(D1 - D2)^2$.

According to this assumption, the creation of the corrected COMPO mode in the direction x should follow the algorithm

$$\text{COMPO}_{(x)} = (D1 + D2) - \alpha(D1 - D2)^2 \quad (2)$$

where: $D1$, $D2$ are the BSE signals from the detectors arranged as in Fig. 1, α is the correction coefficient of the COMPO mode, chosen experimentally (Fig. 2).

Due to the topographic character of the correction term in Eq. (2), the correction of the COMPO mode, both in x and y directions, has been applied (Fig. 1). It means that the algorithm for the COMPO_(xy) mode has been created basing on BSE signals from the detectors aligned both in the x and y axes:

$$\text{COMPO}_{(xy)} = [(D1 + D2) - \alpha(D1 - D2)^2] + [(D3 + D4) - \alpha(D3 - D4)^2]. \quad (3)$$

The efficacy of the proposed method of separation has been shown on the example of scratched wolfram and molybdenum surfaces (Fig. 2). In Figure 2a the surfaces of both metals scratched with the use of an iron blade in the TOPO mode can be seen.

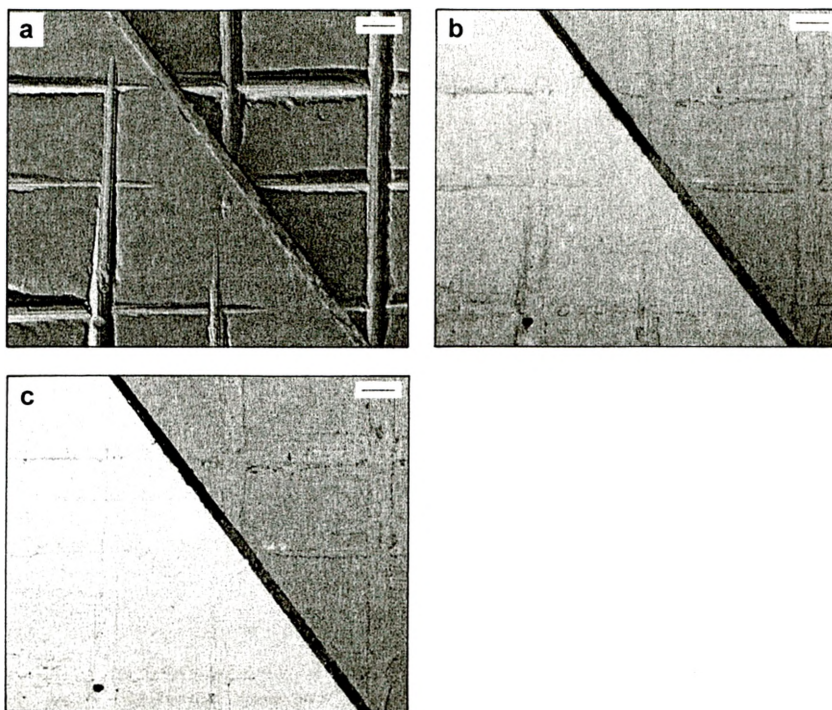


Fig. 2. Comparison of the images of scratched wolfram and molybdenum surfaces (at the right hand side) in the modes of: **a** – TOPO, **b** – COMPO, **c** – $\text{COMPO}_{(\text{xy})} = [(D1 + D2) - 0.05(D1 - D2)^2] + [(D3 + D4) - 0.05(D3 - D4)^2]$. Marker = 50 μm .

In Figures 2b and 2c the images of specimen composition obtained in a traditional way and after employing the correction of the COMPO mode are presented. The comparison of the images shown in Fig. 2a in the TOPO mode and Fig. 2c in the corrected COMPO mode lets us draw the conclusion about the sites at which the topography disturbs the correct analysis of specimen composition. The material analysis with the use of a digital method of colour simulation (which will be described in more details below) has shown that in the place of the scratches there are black areas of rust from the iron blade.

3. Linearization of $\eta = f(Z)$ characteristic

In the previous publication [10], the method of an increase in SEM resolution for the BSE signal by the use of digital image processing has been proposed. The brightness level J of the digital image in the COMPO mode depends on the atomic number Z of the element. The dependence $J = f(Z)$ obtained using the semiconductor detector has been compared with the backscattering coefficient η in Fig. 3 (experimental data after [9]).

During the examination of material composition of an unidentified specimen, at first the calibration of image brightness distribution in the COMPO mode should be

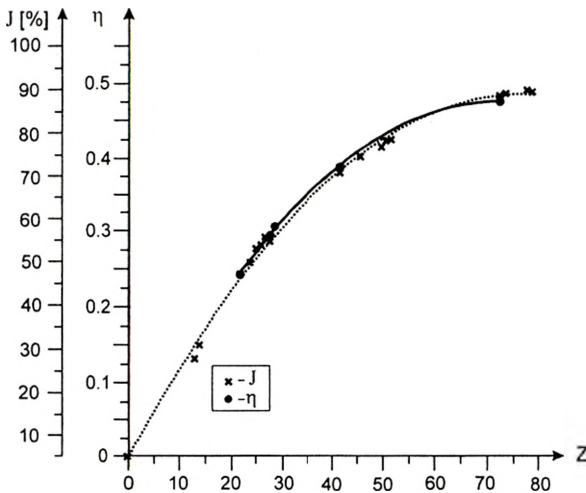


Fig. 3. Calibration of the brightness distribution J for $\eta = f(Z)$ characteristics.

done, in relation to $\eta = f(Z)$ characteristics. For this purpose, the test specimen with at least two elements with identified atomic number is necessary. SEMs are often equipped with the kind of a test specimen, consisting of drops of pure metal. Thus, to the particular values of atomic number, appropriate shadows of image greyness can be related.

The designed computer program enables recounting of brightness at all points of the digital image from the bit value into the η ratio and allows the linearization of the $\eta = f(Z)$ characteristics for high atomic number [10]. The function approximating the experimental $\eta = f(Z)$ dependence was determined by the numerical methods.

The method facilitates distinguishing between intermediate values of the atomic numbers (alloys, material phases). This problem was also reported by BALL and MCCARTEY [7] or CASTAING [26].

The proposed method can be used simultaneously with other methods of the digital presentation of specimen composition. For example, it is possible to enhance the visual resolution in the case of the COMPO image by appropriate colour assignment for different atomic numbers.

4. Method of colour simulation

Commonly available software, like Photo Shop, Photo Paint, Picture Publisher, for digital images processing, gives quite extended possibilities of improving the image quality and its colouring. However, the direct application of such software in the analysis of microscopic images involves the risk of uncontrolled change in information about the specimen examined with the BSE signal. In the analysis of microscopic images, the procedures which interfere in bitmaps should be avoided.

High class scanning electron microscopes are equipped with professional software for acquiring the colour documentation of measurement results. Unfortunately, they are very expensive.

The developed method of colour simulation assigns, in a controlled way, appropriate colours to the areas with different atomic numbers which in the digital image of the specimen in the COMPO mode are represented with different shadows of greyness. However, the simulation of colours can be applied just after carrying out the correction of the COMPO mode [23] and linearization of $\eta = f(Z)$ characteristics [10].

The method of the material composition analysis with the BSE signal has been presented on the example of a specimen consisting of metals with different atomic numbers. A weld of W($Z = 74$)-Mo($Z = 42$) was made with the electron beam with power of 870 W and the welding site was ground off.

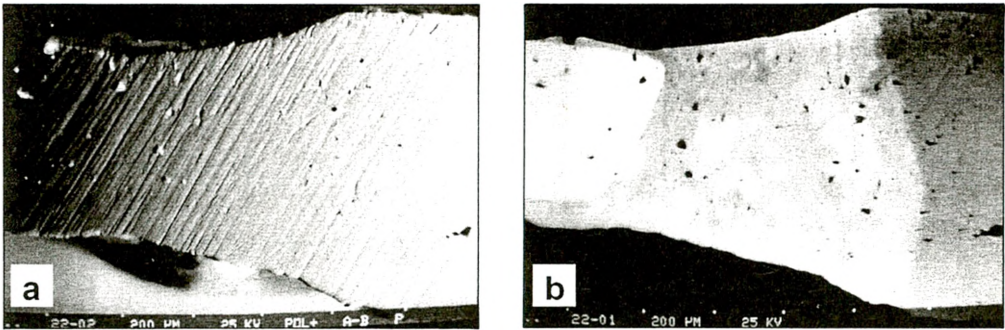


Fig. 4. Microscopic images of W-Mo weld: a – in the TOPO mode, b – in the COMPO mode. Marker = 200 μm .

In Figure 4a the microscopic image of the specimen surface in the TOPO mode has been shown. The sum of signals from four semiconductor detectors placed at high angles with respect to the specimen surface has been used for obtaining the material contrast (Fig. 4b). The beam energy was 20 keV.

In Figure 5a, the image of a fused zone W-Mo from the wolfram side in the COMPO mode (after correction and linearization) has been shown. The digital image has been taken with 8 bit greyness scale resolution and the size of 1200×1000 pixels. From the distribution of greyness shadows at the weld site it can be concluded that the primary materials W and Mo have been mixed under the influence of energetic electron beam.

To the atomic numbers $40 < Z < 76$ colours have been assigned according to the colour scale shown at the bottom part of Fig. 5b. At the weld site, green colour prevails, which suggests high contribution of molybdenum in the alloy. The green section on the scale has been divided into four equal parts and new colours have been assigned to each of them (Fig. 5c). Now, the green colour has been replaced by the pink one, corresponding to the narrower range of atomic numbers. On the other hand, in Fig. 5d the white colour prevails in

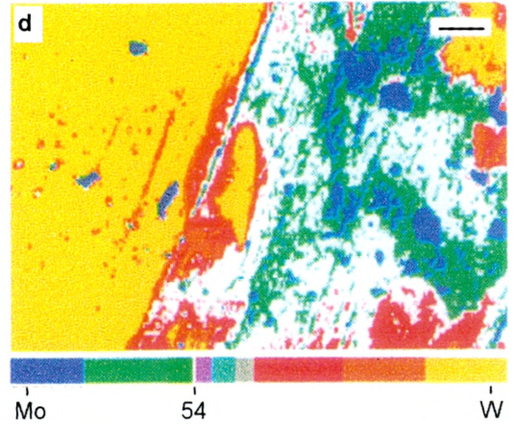
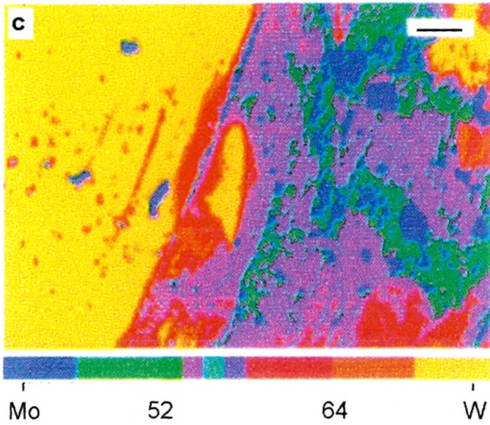
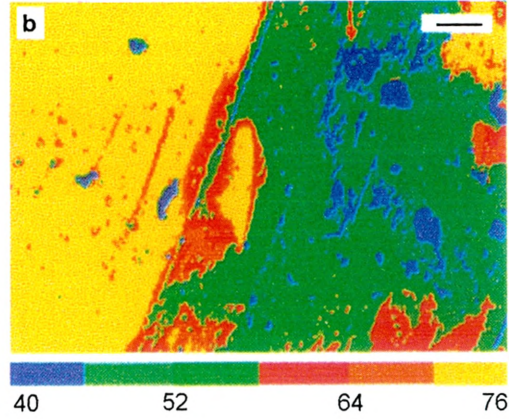
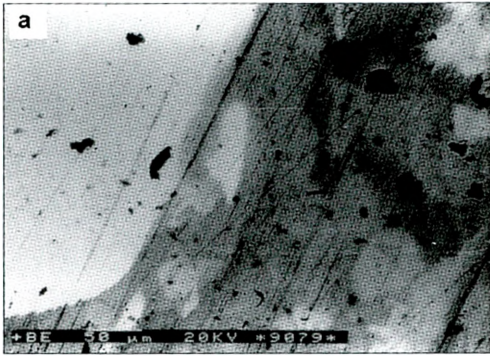


Fig. 5. Images in the COMPO mode of the section of the fusion zone of W-Mo: a – SEM image near wolfram; b, c, d – digital images after the application of COMPO mode correction, linearization of $\eta = f(Z)$ characteristics and colours simulation according to the scale placed below. Marker = 50 μm .

the weld area, what means that there exists the alloy with the averaged atomic number $Z = 54$. This corresponds to molybdenum content of 67%.

In the BSE method the measured atomic number of binary phases has been used to determine the relative concentrations of these components. One ought to mention that the proposed method is valid only for a binary system. In the case when a specimen consists of more than two elements we cannot determine the percentage contribution of every single element separately, but only can identify the alloy with an averaged atomic number.

5. Verification

The results were verified by the use of a conventional method employed in metallography. The weld of Mo-W forms a solid solution in the whole concentration range. The balanced system can exist on condition that the cooling down is slow enough to prevent the diffusion which could compensate for the effects of differences in the concentrations of both components. Solidification of the alloy following electron beam welding runs in unbalanced conditions in a very violent way, which results in slowing down of the diffusion and non-homogeneous concentration of the components at different sites of the weld.

Heterogeneity of composition results in undesirable heterogeneity of the mechanical properties of the weld. The knowledge about the alloys structure lets us take some measures in order to obtain homogenisation of the weld composition (for example by heat treatment). Therefore, the properties of such a specimen are examined by typically employed methods (for example, by the X-ray microanalysis).

Metallographic examination of the specimen has proved the macrostructure typical of the welded joint, *i.e.*, wide heat-affected zone and heterogeneous and coarse-grained weld with a clearly marked outline of a weld junction (Fig. 6).



▲ Fig. 6. Macrostructure of weld of W-Mo. Magnification $30\times$.

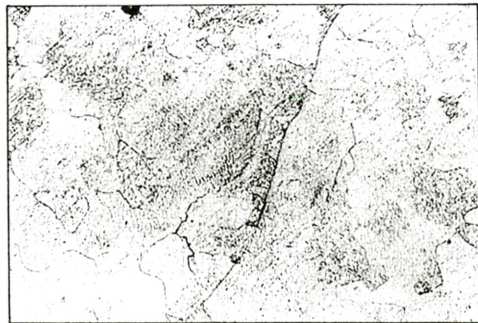


Fig. 7. Fusion zone of wolfram in W-Mo weld. The grains grow on the partially melted crystals of native material (wolfram). Magnification $200\times$.

In the weld area, a zone adjacent to molybdenum fusion into the weld, consisting of partially melted crystals of native material in the form of large grains of crystallites, can be distinguished. In the remaining part of the weld the size of grains slightly decreases and the structure becomes more heterogeneous. In the fused zone from the wolfram side, there can be seen a clearly distinguished division line between the weld and wolfram with characteristic columnar crystals, whose crystallization has started at the partially melted wolfram grains (Fig. 7). In the weld area, inside the particular grains of the weld, crystallization typical of unbalanced condition (dendrites segregation) took place.

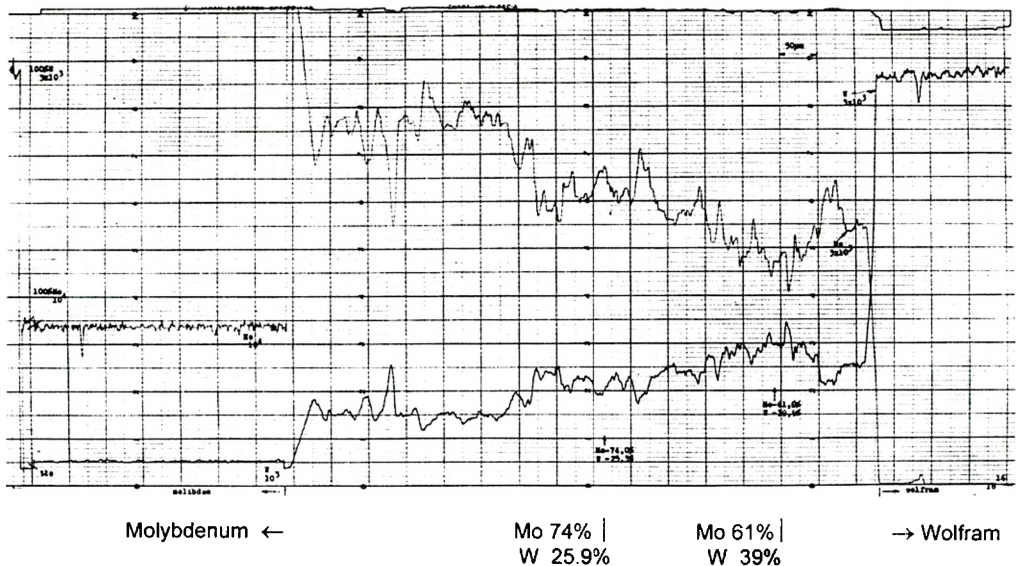


Fig. 8. Linear distribution of molybdenum and wolfram in the weld of W-Mo joint, obtained by the X-ray microanalysis.

The X-ray method is very helpful for the verification of BSE results. The X-ray microanalysis of the Mo-W weld enabled us to determine the composition of the weld and confirmed the observations about the heterogeneity of the weld in particular areas of the joint (Fig. 8). Molybdenum prevails in the weld. However, its content decreases from 80% at the weld zone from the molybdenum side to 61% at the weld zone in the vicinity of wolfram.

6. Conclusions

An improved method of material composition analysis of a specimen in a typical SEM with the BSE signal has been presented and verified. The method can be competitive with the other ones.

For example, BALL and MCCARTNEY [7] showed that in the case of the examination of material with low atomic number the BSE signal allows a ten-times better resolution than the X-ray method.

Basing on numerous tests it can be claimed that the BSE signal applied in the analysis of specimen composition has the following advantages:

- high resolution, particularly in the case of low atomic numbers ([6], [7], [27]),
- possible application for the examination of elements and components with low atomic numbers ([4], [28]),
- possible visualization of composition maps with the simultaneous presentation of the specimen topography ([1], [22]).

References

- [1] KODAKA T., MORI R., DEBARI K., TAKIGUCHI R., HIGASHI S., *Scanning Microsc.* **9** (1995), 907.
- [2] MISHIMA H., SAKAE T., KOZAWA Y., *Scanning Microsc.* **9** (1995), 797.
- [3] GELLER J.D., *Materials Characterization*, Elsevier Sci. Publ. Co. **27** (1991), 199.
- [4] JOY D.C., *Microscopy*, Pt 2, **161** (1991), 343.
- [5] ROSCHGER P., PLENK H., KLAUSHOFER K., ESCHBERGER A., *Scanning Microsc.* **9** (1995), 75.
- [6] VAJDA E.G., SKEDROS J.G., BLOEBAUM R.D., *Scanning Microsc.* **9** (1995), 741.
- [7] BALL M.D., MCCARTNEY D.G., *J. Microsc.*, Pt 1, **124** (1991), 57.
- [8] RAU E.L., SCHINDLER B., REIMER L., [In] *Proc. 11 European Congress on Electron Microscopy, EUREM '96, Part I, 1996*, 336 (published by UCD, Belfield, Dublin, Ireland).
- [9] NIEDRIG H., *J. Appl. Phys.* **53** (1982), R15.
- [10] KACZMAREK D., *Scanning* **19** (1997), 310.
- [11] KACZMAREK D., MULAK A., DOMARADZKI J., *Scanning* **23** (2001), 144.
- [12] ROBINSON V., *Scanning Microsc.* **1** (1996), 107.
- [13] RUSS J.C., *Materials Characterization*, Elsevier Sci. Publ. Co., **27** (1991), 185.
- [14] VALE S.H., [In] *Proc. EMAG '91, Inst. Phys. Conf. Ser. 119* (1991), 193 (IOP Publ. Ltd., Bristol).
- [15] KONKOL A., *Scanning* **18** (1996), 13.
- [16] RADZIMSKI Z.J., *J. Computer-Assisted Microscopy* **6** (1994), 149.
- [17] REIMER L., *Electron Beam Interactions with Solids*, Scanning Electron Microscopy Inc., AMF O'Hare, New York 1984, p. 299.
- [18] KACZMAREK D., *Vacuum* **62** (2001), 303.
- [19] MITYUKHLYAEV V.B., DYUKOV V.G., *Scanning* **16** (1994), 6.
- [20] WALTHER P., AUTRATA R., CHEN Y., PAWLEY J.B., *Scanning Microsc.* **5** (1991), 301.
- [21] KACZMAREK D., KORDAS L., *Beitr. Elektronenmikroskop. Direktabb. Oberf.* **27** (1994), 99.
- [22] WASSINK D.A., RASKI J.Z., LEVITT J.A., HILDRETH D., LUDEMA K.C., *Scanning Microsc.* **5** (1991), 919.
- [23] KACZMAREK D., *Opt. Appl.* **27** (1997), 161.
- [24] KOTERA M., YAMAGUCHI S., FUJIWARA T., SUGA H., *Jpn. J. Appl. Phys.* **31** (1992), 4531.
- [25] MURATA K., *Phys. Status Solidi A* **36** (1976), 197.
- [26] CASTAING R., *Adv. X-ray Analysis* **4** (1960), 351.
- [27] KONKOL A., WILSHAW P.R., BOOKER G.R., *Ultramicroscopy* **55** (1994), 183.
- [28] SHAH J., DURKIN R., [In] *Proc. EMAG '91, Inst. Phys. Conf. Ser. 119* (1991), 161 (IOP Publ. Ltd., Bristol).